

## Photoelectron generation and capture in the resonance fluorescence of a quantum dot

A. Kurzman, A. Ludwig, A. D. Wieck, A. Lorke, and M. Geller

Citation: [Applied Physics Letters](#) **108**, 263108 (2016); doi: 10.1063/1.4954944

View online: <http://dx.doi.org/10.1063/1.4954944>

View Table of Contents: <http://scitation.aip.org/content/aip/journal/apl/108/26?ver=pdfcov>

Published by the [AIP Publishing](#)

---

### Articles you may be interested in

[Charge state control in single InAs/GaAs quantum dots by external electric and magnetic fields](#)

Appl. Phys. Lett. **105**, 041109 (2014); 10.1063/1.4891828

[Polarization-resolved resonant fluorescence of a single semiconductor quantum dot](#)

Appl. Phys. Lett. **101**, 251118 (2012); 10.1063/1.4772495

[Voltage-controlled electron tunneling from a single self-assembled quantum dot embedded in a two-dimensional-electron-gas-based photovoltaic cell](#)

J. Appl. Phys. **110**, 053110 (2011); 10.1063/1.3633216

[Multiexciton complexes in InAs self-assembled quantum dots](#)

J. Appl. Phys. **105**, 122406 (2009); 10.1063/1.3117231

[Optical properties of single InAs quantum dots in close proximity to surfaces](#)

Appl. Phys. Lett. **85**, 3423 (2004); 10.1063/1.1806251

---

The advertisement features a blue background with a glowing light effect. On the left, there is a small image of the 'AIP Applied Physics Reviews' journal cover, which shows a diagram of a quantum dot structure. The main text 'NEW Special Topic Sections' is written in large, white, bold letters. Below this, the text 'NOW ONLINE' is in yellow, followed by 'Lithium Niobate Properties and Applications: Reviews of Emerging Trends' in white. The AIP Applied Physics Reviews logo is in the bottom right corner.

**NEW Special Topic Sections**

**NOW ONLINE**  
Lithium Niobate Properties and Applications:  
Reviews of Emerging Trends

**AIP** Applied Physics  
Reviews

## Photoelectron generation and capture in the resonance fluorescence of a quantum dot

A. Kurzmann,<sup>1,a)</sup> A. Ludwig,<sup>2</sup> A. D. Wieck,<sup>2</sup> A. Lorke,<sup>1</sup> and M. Geller<sup>1</sup>

<sup>1</sup>Fakultät für Physik and CENIDE, Universität Duisburg-Essen, Lotharstraße 1, Duisburg 47048, Germany

<sup>2</sup>Chair of Applied Solid State Physics, Ruhr-Universität Bochum, Universitätsstr. 150, 44780 Bochum, Germany

(Received 6 April 2016; accepted 16 June 2016; published online 28 June 2016)

Time-resolved resonance fluorescence on a single self-assembled quantum dot (QD) is used to analyze the generation and capture of photoinduced free charge carriers. We directly observe the capture of electrons into the QD as an intensity reduction of the exciton transition. The exciton transition is quenched until the captured electron tunnels out of the dot again in the order of milliseconds. Our results demonstrate that even under resonant excitation, excited free electrons are generated and can negatively influence the optical properties of a QD. *Published by AIP Publishing.*

[<http://dx.doi.org/10.1063/1.4954944>]

Self-assembled quantum dots (QDs) as artificial atoms in a solid-state matrix show almost ideal properties for optical quantum devices. They are perfect building blocks for single photon sources<sup>1–3</sup> with a high quantum efficiency<sup>4</sup> and high photon indistinguishability.<sup>5–7</sup> These optical properties arise from very stable exciton transitions.<sup>8,9</sup> However, the ultimate goal of a transform-limited photon stream has not yet been reached, as spectral wandering of the center frequency of the QD transition is still observed. The major sources of this spectral jitter are charge and nuclear spin noise.<sup>10,11</sup> Charge noise can arise from charging/discharging of trap states that were filled by photoexcited free charge carriers.<sup>12</sup> Furthermore, these photoexcited electrons can relax into the QD, quenching the transitions in a resonant measurement,<sup>13,14</sup> as demonstrated for QDs in a micro-cavity without an electrical gate contact and in nitrogen vacancy centers in diamond.<sup>15</sup> The generation of these free, excited charge carriers and its influence on the optical properties of a single QD has so far not been studied in optical measurements on electrically tunable QDs.<sup>16</sup>

We show here in a time-resolved resonance fluorescence (RF) measurement<sup>17,18</sup> that free charge carriers are generated by photoexcitation from the charge reservoir in a resonant or near resonant measurement. These carriers can be captured by the QD, which can be observed by a quenching of the exciton transition. In diode structures where the QDs are separated by a tunneling barrier from the charge reservoir, this effect has not been observed before, as the probability for a capture process of such an electron into the dot is orders of magnitude lower than the average tunneling rate between reservoir and dot.<sup>19,20</sup> This means that the captured electron is emitted swiftly by tunneling to the charge reservoir; hence, its influence on the exciton transition is difficult to discern. We show here that there is always a photoinduced generation of charge carriers, and we are able to observe this process in a device that has tunneling times in the order of milliseconds; more than 6 orders of magnitude slower than the exciton recombination time. These photoelectrons are excited

from the highly doped back contact, can relax to the QD layer, and influence its optical properties negatively.

The investigated sample was grown by molecular beam epitaxy (MBE) and resembles a Schottky diode with a layer of self-assembled InAs QDs. In detail, a 300 nm GaAs layer was deposited on a semi-insulating GaAs substrate, followed by a 50 nm silicon-doped GaAs layer, which forms the electron reservoir. A tunneling barrier, consisting of 30 nm GaAs, 10 nm Al<sub>0.34</sub>Ga<sub>0.66</sub>As, and 5 nm GaAs, was grown. This layer separates the InAs QDs from the doped back contact. The InAs QDs were formed by growing 1.6 monolayers of InAs partially capped by 2.7 nm GaAs and flushed at 600 °C for 1 min to shift the emission wavelength to  $\approx$ 950 nm. They were further capped by a 27.5 nm GaAs layer, a 140 nm superlattice (35 periods of 3 nm AlAs and 1 nm GaAs), and 10 nm GaAs. The Ohmic back contact was formed by AuGe and Ni evaporation and annealing. Transparent Schottky gates were prepared on the sample surface by standard optical lithography and deposition of 7 nm NiCr. On top of these gates, a zirconium solid immersion lens (SIL) was mounted to improve the collection efficiency of the QD emission.<sup>21</sup> A gate voltage, applied between the top gate and the Ohmic back contact, induces an external electric field and controls the charge state in the QD.<sup>22,23</sup>

We use a confocal microscope setup in a bath-cryostat at a temperature of 4.2 K. For the RF measurements, the exciton ( $X$ ) or trion ( $X^-$ ) transitions are driven resonantly by a linearly polarized and frequency stabilized tunable diode laser. In a confocal geometry, both laser excitation and QD emission are guided along the same path using a 10:90 beam-splitter. Single QD resolution is achieved by a 0.65 NA objective lens in front of the above mentioned SIL, resulting in a spot size of 1  $\mu$ m. The emission of the QD is collected behind a polarizer, which is polarized orthogonally to the excitation laser and suppresses the laser light by a factor of  $10^7$ . The RF signal of the QD is detected by an avalanche photo diode (APD) and is recorded using a time-to-digital converter with a time resolution of 81 ps.

Figure 1(a) shows a map of the RF intensity versus laser frequency and gate voltage. We observe the exciton

<sup>a)</sup>Electronic mail: annika.kurzmann@uni-due.de

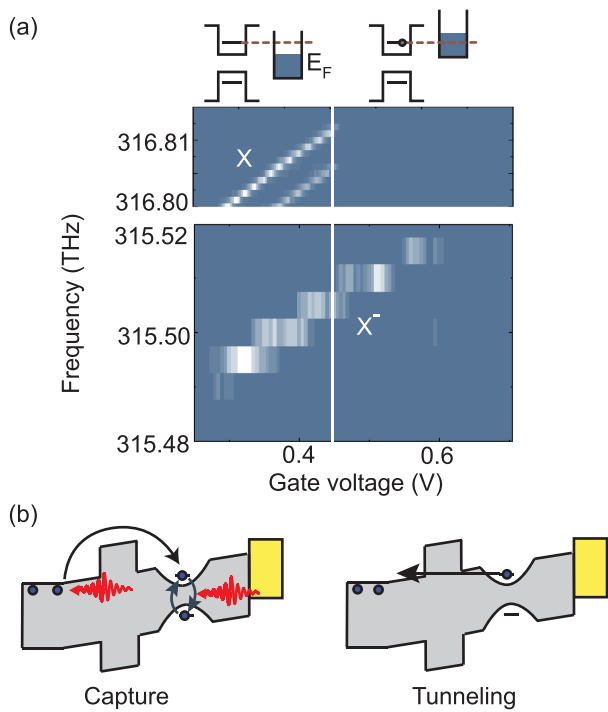


FIG. 1. (a) RF of the exciton and trion transition for different laser excitation frequencies and gate voltages. The trion transition is observed for gate voltages where tunneling into the QD is energetically forbidden. (b) Schematic illustration of the involved processes of generation, capture, and tunneling of the optically excited free electrons.

transition (X) with its fine structure splitting<sup>24</sup> and the quantum confined stark effect.<sup>25</sup> The exciton is observed for gate voltages below 0.45 V. At this gate voltage, the Fermi energy  $E_F$  of the back contact is in resonance with the first QD level and tunneling of electrons into the QD is energetically allowed. For higher gate voltages, the QD will be singly charged and the trion transition is observed for a laser frequency of about 315.51 THz. Surprisingly, we also observe the trion transition below 0.45 V for high laser excitation powers, even though the tunneling of electrons from the back contact into the QD is energetically forbidden.<sup>16</sup> We can explain this result by the capture process of optically generated, free excited electrons from the back contact into the dot states, as schematically illustrated in Fig. 1(b) left. These electrons are generated by the laser that is used for the resonant excitation and can diffuse to the QD layer and charge the QD even at gate voltages where the tunneling is energetically forbidden. A QD charged with one electron cannot be excited on the exciton transition until the electron tunnels back to the charge reservoir, as shown in the right hand side of Fig. 1(b). Note, in addition, that we observe the trion transition with a much smaller intensity than the exciton transition, which can be explained by the strong influence of the Auger recombination in QD structures with thick tunneling barriers.<sup>26</sup>

We can directly observe the capture of electrons into the QD in a time-resolved two color n-shot measurement, demonstrated in the following. The first laser drives the exciton transition resonantly at a frequency of 317.803 THz with a constant, very low laser intensity (blue line in Fig. 2(a)), so that no free charges are generated and captured by the dot. To demonstrate that the generation of free electrons is a

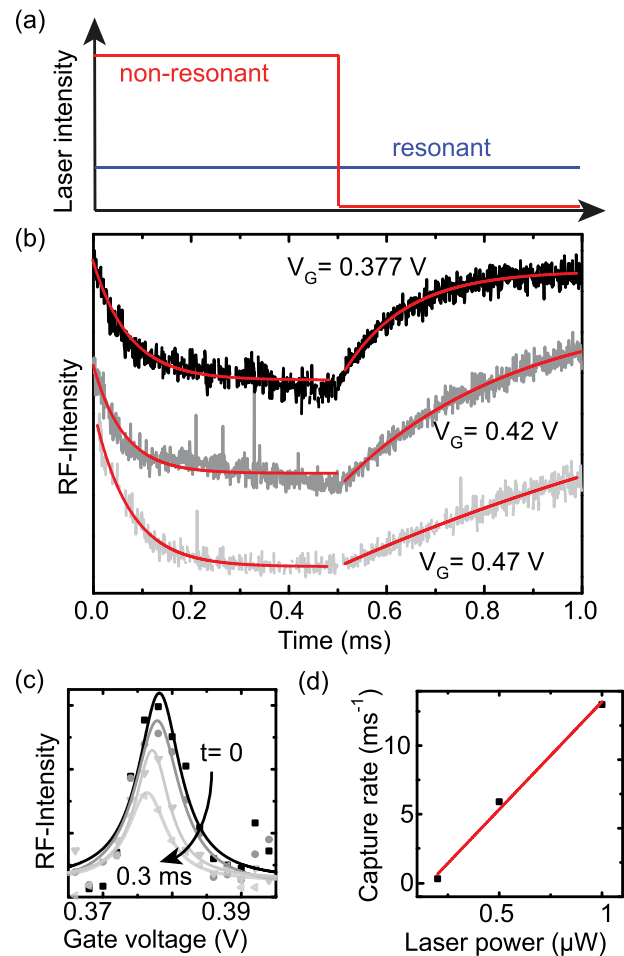


FIG. 2. (a) Intensities of the two different lasers for the time-resolved RF measurement. The exciton transition is excited resonantly with constant intensity during the measurement. A second laser with a frequency close to the resonance is pulsed with high intensity. (b) Time-resolved RF of the exciton transition for different gate voltages. The RF-signal is quenched when the non-resonant second laser is turned on. The signal increases again after switching the second laser off. (c) Evolution of the Lorentzian line shape of the exciton transition after a second non-resonant laser is turned on for a duration of  $t = 0, 0.03, 0.06, 0.15,$  and  $0.3$  ms. A suppression of the intensity and an energy shift is observed. (d) Capture rates of electrons into the QD for different, non-resonant laser intensities.

non-resonant effect, we use a second laser with a frequency of 319.67 THz. This rules out any band-to-band transition. The second laser is used with a pulsed laser intensity that is two orders of magnitude higher than the intensity of the resonant laser. It is switched on at  $t = 0$  (see Fig. 2(a), red line) and off at  $t = 0.5$  ms. We repeat this measurement for different detunings between the first laser and the exciton energy, so that the Lorentzian line shape of the exciton transition is observed for different times in Fig. 2(c). An intensity reduction and a shift of the maximum of the exciton transition are measured up to a time delay of 0.3 ms. The time evolution of the maximum intensity is shown in Fig. 2(b). We observe an exponential decay after the laser is switched on at  $t = 0$  with a relaxation rate of  $13 \text{ ms}^{-1}$  (determined from an exponential fit to the data, see red line). The steady state intensity at  $t = 0.5$  ms is about 30% of the intensity at  $t = 0$ , and it is given by the interplay between electron capture and tunneling. The capture rate can be easily tuned by the laser excitation power, leading to a change in the overall relaxation rate,

as shown in Fig. 2(d). We find a linearly increasing capture rate (solid red line) with increasing laser power, as expected for optically excited electrons in the vicinity of the dot.

In addition to a quenching of the exciton transition, we observe in Fig. 2(c) a shift of the Lorentzian line to lower gate voltages with increasing time duration. This effect has been observed in optical measurements on QDs without an electrical gated structure and can be explained by trapped charges in the vicinity of the dot.<sup>12</sup>

The tunneling rate of electrons out of the dot can be observed for  $t > 0.5$  ms in Fig. 2(b). After the non-resonant laser is turned off and the photogeneration of electrons ceases, an exponential increase of the exciton RF intensity is observed. Increasing the gate voltage from  $V_G = 0.377$  V to 0.47 V, we observe that the tunneling rate decreases from  $7.8 \text{ ms}^{-1}$  down to  $1.2 \text{ ms}^{-1}$  (Fig. 2(b)). We have determined these rates by fitting the tunneling transients exponentially (solid red lines in Fig. 2(b)) and plotted the values versus gate voltage in Fig. 3. The tunneling rates decrease with increasing gate voltage as the tunneling barrier is increased and its transparency is reduced (Fowler–Nordheim tunneling). We calculated the transparency of the barrier  $T$  using the WKB approximation<sup>27</sup> and determined the tunneling rate by  $\gamma = Tf$  where  $f$  is the attempt frequency. The attempt frequency here is a phenomenological fit parameter ( $f = 349 \text{ ns}^{-1}$ ), and it only influences the magnitude of the tunneling rates. The calculation is in very good agreement with the data points in Fig. 3. This demonstrates two things: (i) The observed transients in Fig. 2(b) for  $t > 0.5$  ms is caused by electron tunneling out of the QD. (ii) More importantly, the quenching of the RF signal for  $t < 0.5$  ms is a consequence of electron capture into the dot states, which shifts the resonance frequency from the exciton to the trion transition. In sub-bandgap excitation, this is possible by photoinduced excitation of free electrons from the highly doped back contact and subsequent capture in the dot states.

Finally, with another pulsed RF measurement, we are able to determine the tunneling rate into the QD without the influence of the photoinduced electron capture. We use a pulsed resonant excitation on the exciton transition in combination with a pulsed gate voltage (Fig. 4(a)) in a situation where an electron will tunnel into the dot and quench the exciton transition. The gate voltage controls the tunneling

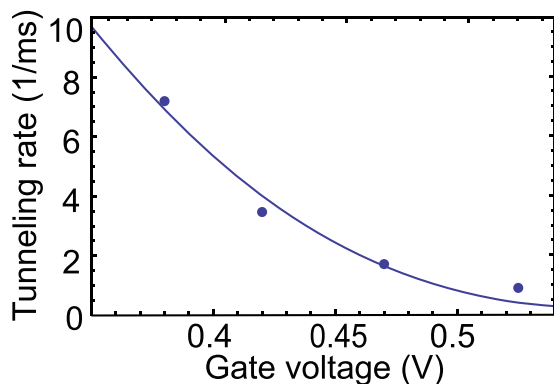


FIG. 3. Measured tunneling rates for different gate voltages together with a fit to the data using the WKB approximation for the transparency of the tunneling barrier.

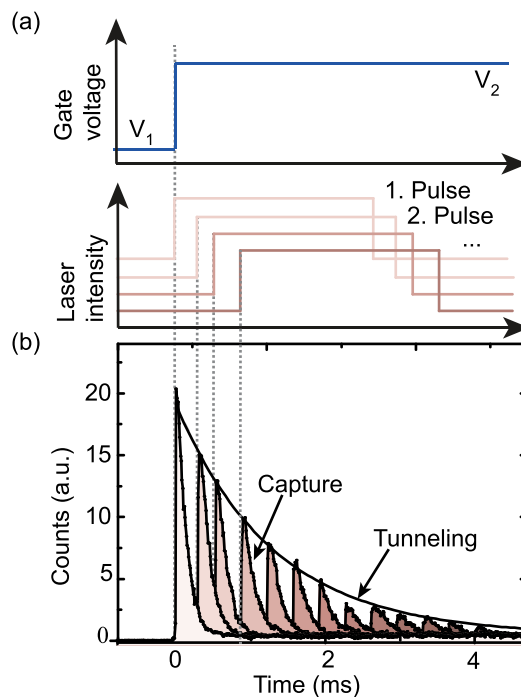


FIG. 4. (a) Upper panel: Pulsed gate voltage. Without illumination, for  $V_1$  the QD is uncharged, while for  $V_2$  the QD gets charged. Lower panel: Pulsed laser intensity with different time delays used for the measurement in (b). (b) Time dependent RF-signal with a pulsed gate voltage and a pulsed laser intensity revealing both electron tunneling and the capture of photo generated electrons.

while the pulsed laser switches on the photoinduced electron generation and probes the RF signal from the exciton. In detail, we first prepare an empty QD state by setting the gate voltage to  $V_1 = 0$  V, a value well below the steady-state tunneling voltage at 0.45 V (see also Fig. 1(a)). The laser energy is adjusted so that RF will occur for a gate voltage  $V_2 = 0.525$  V, which lies above the tunneling voltage. At  $t = 0$ , the gate voltage is switched to  $V_2$  and shifts the QD exciton transition into resonance with the laser. A strong RF signal is visible at  $t = 0$  in Fig. 4(b). The transition is now quenched by the two possible processes: (i) capture of photoinduced electrons and (ii) electron tunneling into the QD. For the chosen laser intensity, the capture is faster than the tunneling; hence, for different time delays after the voltage pulse, we observe this process as a fast exponential decay in the shaded curves in Fig. 4(b). At the start of each laser pulse, a strong RF intensity is visible as the electron capture has not set in yet. The maximum RF intensity for different time delays reflects the probability for tunneling, which is visualized by the solid black line in Fig. 4. We are able to determine the tunneling rate into the dot to be  $1 \text{ ms}^{-1}$  from this envelope function. This rate is a factor of two larger than the tunneling out process for the same gate voltage and, hence, in qualitative agreement with the all-electrical measurements.<sup>28</sup>

In conclusion, we have shown that in resonant measurements (like RF and differential reflection) free, excited charge carriers are generated by excitation from a doped back contact. These charge carriers can be captured into the dot states and quench the exciton transition for a time duration that is given by the average tunneling time out of the



dot. This effect should also be present in samples with small tunneling barriers, where quenching of the exciton transition is not observed. However, it could lead to an increased line-width due to the photoinduced electron in the vicinity of the dot and inside the dot. This possible influence on the line-width needs further investigations in the future.

- <sup>1</sup>Z. Yuan, B. E. Kardynal, R. M. Stevenson, A. J. Shields, C. J. Lobo, K. Cooper, N. S. Beattie, D. A. Ritchie, and M. Pepper, *Science* **295**, 102 (2002).
- <sup>2</sup>A. Kiraz, P. Michler, C. Becher, B. Gayral, L. Zhang, E. Hu, W. V. Schoenfeld, P. M. Petroff, and A. Imamoglu, *Coherence and Quantum Optics VIII* (Springer, 2003) pp. 165–170.
- <sup>3</sup>C. Matthiesen, A. N. Vamivakas, and M. Atatüre, *Phys. Rev. Lett.* **108**, 093602 (2012).
- <sup>4</sup>P. Michler, A. Kiraz, C. Becher, W. V. Schoenfeld, P. M. Petroff, L. Zhang, E. Hu, and A. Imamoglu, *Science* **290**, 2282 (2000).
- <sup>5</sup>C. Santori, D. Fattal, J. Vučković, G. S. Solomon, and Y. Yamamoto, *Nature* **419**, 594 (2002).
- <sup>6</sup>C. Matthiesen, M. Geller, C. H. H. Schulte, C. Le Gall, J. Hansom, Z. Li, M. Hugues, E. Clarke, and M. Atatüre, *Nat. Commun.* **4**, 1600 (2013).
- <sup>7</sup>Y.-J. Wei, Y.-M. He, M.-C. Chen, Y.-N. Hu, Y. He, D. Wu, C. Schneider, M. Kamp, S. Höfling, C.-Y. Lu, and J.-W. Pan, *Nano Lett.* **14**, 6515 (2014).
- <sup>8</sup>A. Kuhn, M. Hennrich, and G. Rempe, *Phys. Rev. Lett.* **89**, 067901 (2002).
- <sup>9</sup>A. V. Kuhlmann, J. H. Prechtel, J. Houel, A. Ludwig, D. Reuter, A. D. Wieck, and R. J. Warburton, *Nat. Commun.* **6**, 8204 (2015).
- <sup>10</sup>A. V. Kuhlmann, J. Houel, A. Ludwig, L. Greuter, D. Reuter, A. D. Wieck, M. Poggio, and R. J. Warburton, *Nat. Phys.* **9**, 570 (2013).
- <sup>11</sup>J. Houel, A. V. Kuhlmann, L. Greuter, F. Xue, M. Poggio, B. D. Gerardot, P. A. Dalgarno, A. Badolato, P. M. Petroff, A. Ludwig, D. Reuter, A. D. Wieck, and R. J. Warburton, *Phys. Rev. Lett.* **108**, 107401 (2012).
- <sup>12</sup>C. Arnold, V. Loo, A. Lemaître, I. Sagnes, O. Krebs, P. Voisin, P. Senellart, and L. Lanco, *Phys. Rev. X* **4**, 021004 (2014).
- <sup>13</sup>H. S. Nguyen, G. Sallen, M. Abbarchi, R. Ferreira, C. Voisin, P. Roussignol, G. Cassabois, and C. Diederichs, *Phys. Rev. B* **87**, 115305 (2013).
- <sup>14</sup>H.-S. Nguyen, G. Sallen, C. Voisin, P. Roussignol, C. Diederichs, and G. Cassabois, *Phys. Rev. Lett.* **108**, 057401 (2012).
- <sup>15</sup>P. Siyushev, H. Pinto, M. Vörös, A. Gali, F. Jelezko, and J. Wrachtrup, *Phys. Rev. Lett.* **110**, 167402 (2013).
- <sup>16</sup>S. Seidl, M. Kroner, P. A. Dalgarno, A. Högele, J. M. Smith, M. Ediger, B. D. Gerardot, J. M. Garcia, P. M. Petroff, K. Karrai, and R. J. Warburton, *Phys. Rev. B* **72**, 195339 (2005).
- <sup>17</sup>C.-Y. Lu, Y. Zhao, A. N. Vamivakas, C. Matthiesen, S. Fält, A. Badolato, and M. Atatüre, *Phys. Rev. B* **81**, 035332 (2010).
- <sup>18</sup>A. Kurzmann, B. Merkel, P. A. Labud, A. Ludwig, A. D. Wieck, A. Lorke, and M. Geller, e-print [arXiv:1505.07682](https://arxiv.org/abs/1505.07682) [cond-mat.mes-hall].
- <sup>19</sup>A. Högele, S. Seidl, M. Kroner, K. Karrai, R. J. Warburton, B. D. Gerardot, and P. M. Petroff, *Phys. Rev. Lett.* **93**, 217401 (2004).
- <sup>20</sup>A. Nick Vamivakas, Y. Zhao, C.-Y. Lu, and M. Atatüre, *Nat. Phys.* **5**, 198 (2009).
- <sup>21</sup>B. D. Gerardot, S. Seidl, P. A. Dalgarno, R. J. Warburton, M. Kroner, K. Karrai, A. Badolato, and P. M. Petroff, *Appl. Phys. Lett.* **90**, 221106 (2007).
- <sup>22</sup>P. M. Petroff, A. Lorke, and A. Imamoglu, *Phys. Today* **54**(5), 46 (2001).
- <sup>23</sup>H. Drexler, D. Leonard, W. Hansen, J. P. Kotthaus, and P. M. Petroff, *Phys. Rev. Lett.* **73**, 2252 (1994).
- <sup>24</sup>D. Gammon, E. S. Snow, B. V. Shanabrook, D. S. Katzer, and D. Park, *Phys. Rev. Lett.* **76**, 3005 (1996).
- <sup>25</sup>S.-S. Li and J.-B. Xia, *J. Appl. Phys.* **88**, 7171 (2000).
- <sup>26</sup>A. Kurzmann, A. Ludwig, A. D. Wieck, A. Lorke, and M. Geller, *Nano Lett.* **16**, 3367–3372 (2016).
- <sup>27</sup>R. J. Luyken, A. Lorke, A. O. Govorov, J. P. Kotthaus, G. Medeiros-Ribeiro, and P. M. Petroff, *Appl. Phys. Lett.* **74**, 2486 (1999).
- <sup>28</sup>A. Beckel, A. Kurzmann, M. Geller, A. Ludwig, A. D. Wieck, J. König, and A. Lorke, *Europhys. Lett.* **106**, 47002 (2014).